Mapping the Distribution of Components in Formulated Polymeric Membranes Using FTIR-ATR Microscopy

Chris Sammon[a], Sabrina Boussetta[a] and Colin Melia[b]*

[a] Materials Research Institute, Sheffield Hallam University, Pond St, Sheffield, S1 1WB, UK
[b] School of Pharmaceutical Sciences, University of Nottingham, University Park, Nottingham, NG7 2RD, UK

Summary: This paper shows how FTIR-ATR microscopy can be used to monitor the distribution of components in polymeric membranes without the need for extensive sample preparation. The validity of the technique is proven using a different technique, namely ESEM. Three examples of its use are given; a drug in a pharmaceutical tablet, a biocide in a PVC formulation and a defect on a polymer coated metal.

Introduction

The ability of vibrational spectroscopy to be used to characterise chemical and morphological differences in a material is well-documented [1]. When coupled to a microscope the techniques become extremely useful tools with high sensitivity and good spatial resolution [2]. Of course, with any conventional microscopic method ultimately spatial resolution is limited by the wavelength of the probing radiation, hence for scanning electron microscopy (SEM) using short wavelength electrons as the probing moiety, very high spatial resolution can be achieved. As the wavelength of the probing radiation increases, so spatial resolution decreases, with FTIR microscopy being limited to the 10's of μm. Despite suffering from poorer spatial resolution compared to say SEM and Raman microscopy, FTIR microscopy is still very popular and useful, as it is both fast and sensitive. Indeed numerous workers are using FTIR microscopy as the tool of choice to solve a host of problems in the polymer and pharmaceutics industries [3-8].

FTIR point mapping is a technique that can readily be used to generate a chemical 'image' of a material. This involves the building up of a mosaic of infrared spectra, at discrete points, to determine the distribution of components across a sample (figure 1).

 CCC 1022-1360/00/$ 17.50+.50/0

Traditionally point mapping has been achieved by carrying out time consuming (several hours) sample preparation, such as microtoming, to make the sample thin enough to allow transmission microscopy [3-7]. But under favourable conditions it is possible to circumvent sample preparation by carrying out FTIR-ATR microscopy.

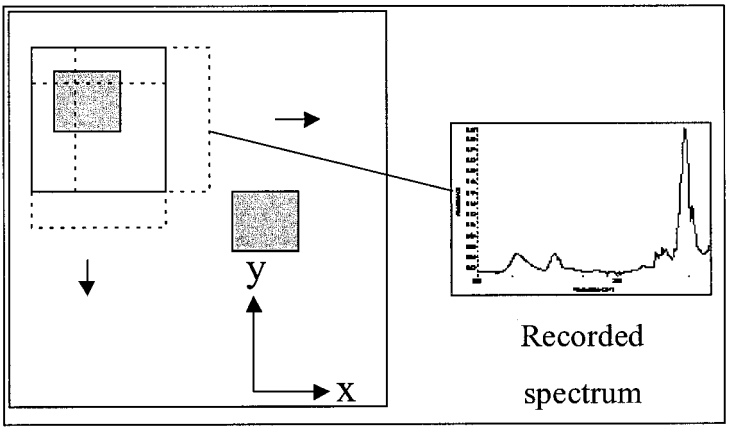

Figure 1 Schematic of the point mapping experiment.

FTIR-ATR is a 'surface' sensitive technique relying on an intimate contact between the ATR crystal and the sample. A detailed description of ATR is given elsewhere [9], but to summarise the sampling depth is controlled by the wavelength of light, the angle of incidence and the refractive indices of the sample and ATR crystal. The sampling depth is related to the penetration depth of the evanescent field (d_p) which can be calculated using equation 1.

$$d_p = \frac{\lambda}{2n_2\pi\sqrt{\sin^2\theta - \left(\frac{n_1}{n_2}\right)^2}} \qquad \text{(Equation 1)}$$

Where

n_1 is the refractive index of the sample

n_2 is the refractive index of the ATR crystal

θ is the angle of incidence

λ is wavelength of the incident radiation

FTIR-ATR microscopy has two main advantages over transmission FTIR microscopy. Firstly, sample preparation can be avoided. Secondly, there is an effective improvement in spatial resolution due to the reduction of the effective wavelength of the infrared radiation by retardation in the high refractive index ATR crystal material [2]. This essentially reduces the sampling aperture by the refractive index of the ATR crystal material. For high refractive index materials such as Si (n_2 = 3.4) and Ge (n_2 = 4) this is a significant improvement of effective resolution. Of course there are also disadvantages, for example when samples show significant topographical features or there is a risk of crystal contamination, the technique cannot be used. There can also be throughput problems that necessitate longer sampling times.

In this paper we highlight three examples of FTIR-ATR microscopy, where heterogeneity across polymeric membranes are characterised.

Instrumentation

All FTIR data was collected using a Spectra Tech Continuμm microscope © coupled to a Nicolet 860 FTIR spectrometer ©. Spectra were recorded at 8 cm^{-1} resolution, averaging 100 scans. The system was fitted with a computer controlled automated stage and all FTIR maps were recorded in auto ATR contact mode. Maps were obtained by collecting spectra at 10 μm intervals with an effective aperture size of ~30 x 30 μm.

Results and Discussion

1 Investigation of the phase separation of a drug in a pharmaceutical tablet

In sustained release tablets the distribution of the active is critical if control of dissolution rates are to be obtained. Release is generally achieved by the matrix forming a soluble/semi-soluble layer in which the active is mobile. Significant phase separation can result in all the active being released at once having an adverse therapeutic effect. One such system where phase separation is known to occur is the antihistamine, chlorpheniramine maleate (20%), in the binding polymer hydroxy propyl methylcellulose (HPMC) [10]. The purpose of this work was to validate the FTIR-ATR microscopy

technique with another unrelated technique. We have used Environmental Scanning Electron Microscopy (ESEM) coupled to an Energy Dispersive X-ray (EDX) analyser to generate 'maps' of the drug in the polymer matrix. The structure of both the drug and the matrix are given in figure 2. In the EDX analysis we can map the heavy chlorine atom to achieve contrast. In FTIR-ATR microscopy, we can use the drug ν_{ring}(CC) and ν(OH) bands as highlighted in figure 2.

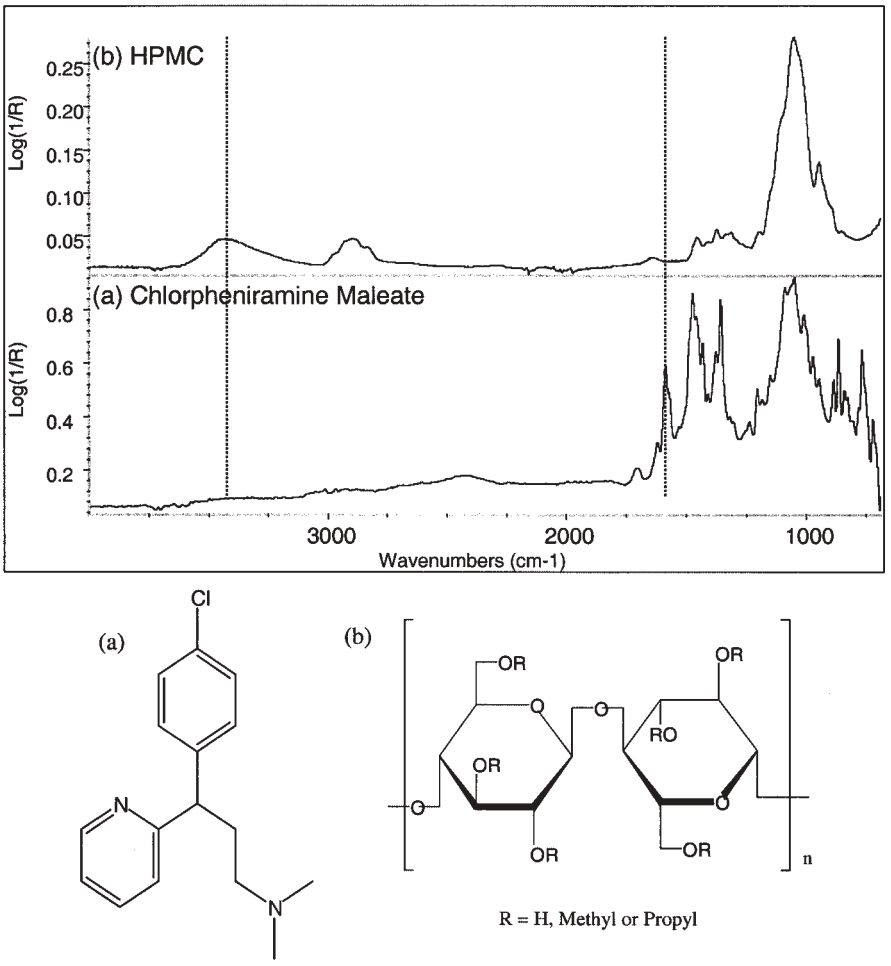

Figure 2. The structure and infrared spectra of (a) drug (chlorpheniramine maleate) and (b) binder (HPMC) used for the validation of the FTIR-ATR technique.

The SEM image and EDX map of Chlorine are shown in figure 3. It is clear that there is good correlation between HPMC crystals in the SEM image and the dark regions in the EDX image (i.e. Chlorine deficient). From this image we can determine the domain sizes to be of the order of 10's → 100's of μm, which is ideal for the FTIR technique. Because of potential beam damage it was not possible to look on the same tablet using FTIR-ATR spectroscopy.

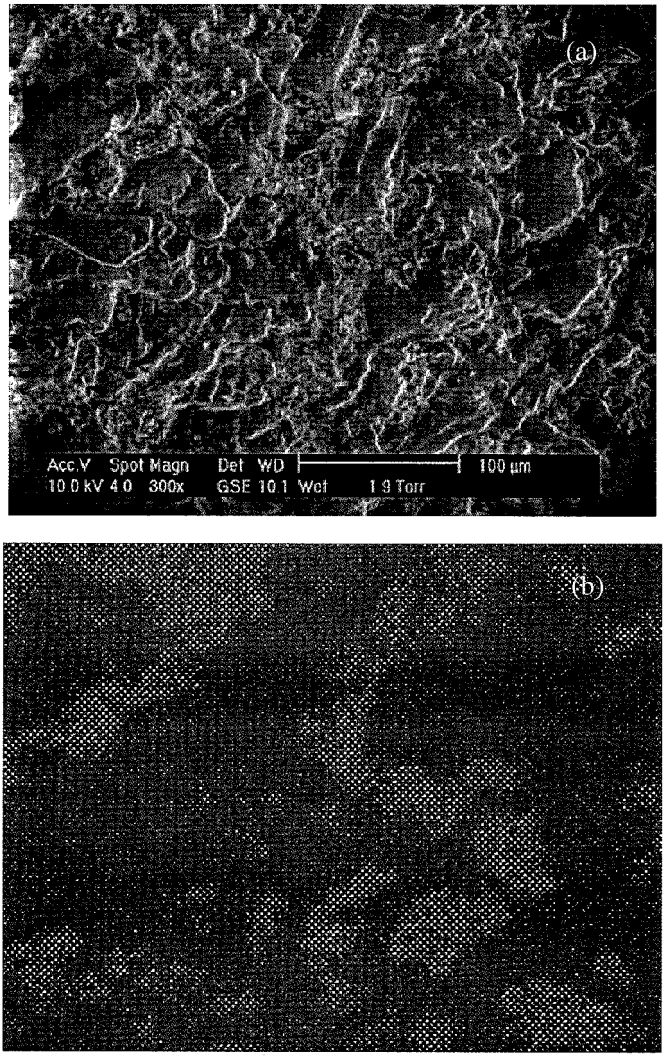

Figure 3. SEM image(a) and EDX map of Chlorine (b) in tablet formulation.

Figure 4 shows clearly that domain sizes for HPMC (4(a)) and drug (4(b)) map on well with the EDX image maps. From figure 4 we can see there is clear contrast between the HPMC and drug regions, confirming phase separation. We can therefore conclude that FTIR-ATR microscopy provides accurate information on domain sizes verified using ESEM-EDX.

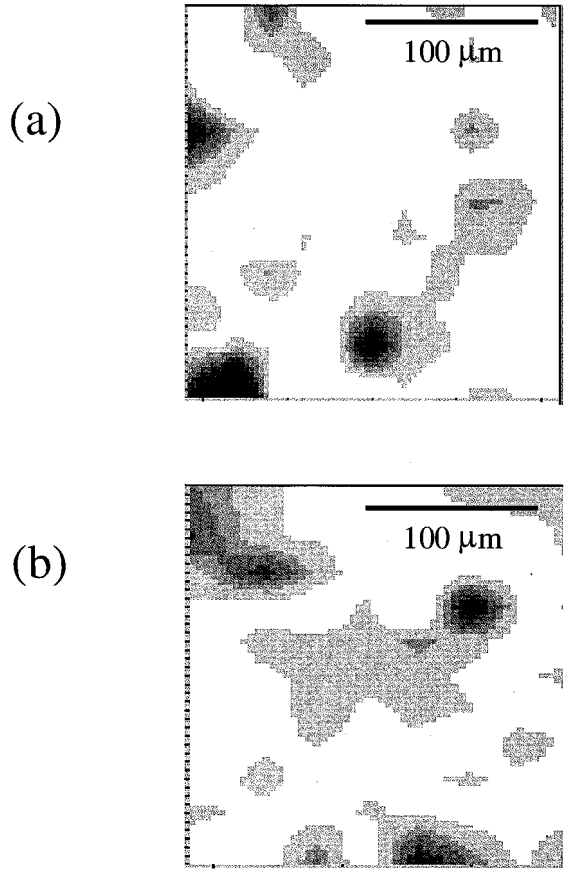

Figure 4. FTIR maps of the surface of a pharmaceutical tablet (a) mapping for the binder, (b) mapping for the drug.

2 Mapping the distribution of additives in a formulated PVC film

The inclusion of additives to improve performance or processability of polymers is common [11]. In this example, we have mapped the distribution components of a PVC film. PVC is a very common polymer, which is cheap to manufacture but which requires the addition of other materials to make it useful. PVC also provides a good environment for microbial growth and without the addition of biocides this can preclude its use in numerous applications such as floor tiling and shower curtain materials [12]. In these applications, the PVC formulation is likely to come into contact with water. There are two issues in this case (i) what is the distribution of biocide in the formulation ? (ii) what happens to the biocide distribution after contact with water ? Work was previously undertaken in our group using Raman microscopy on this system and will be published later. Raman microscopy has better spatial resolution than FTIR microscopy but generally suffers from poorer sensitivity. Initially we wished to verify work done using Raman, but we also wished to look at formulations with lower biocide loadings, which are commonly used in real systems. So biocide loadings of 5% and 0.5% were characterised before and after treatment in water.

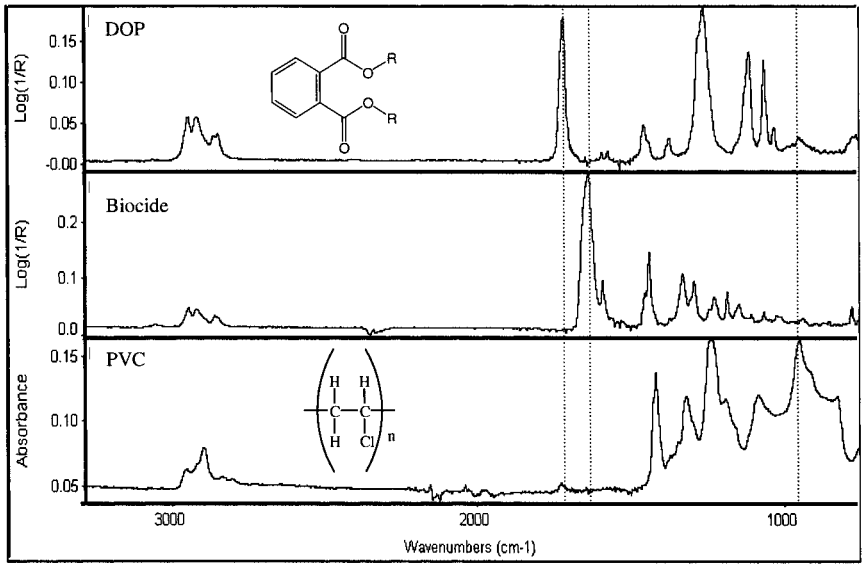

Figure 5. Structures and spectra of raw components of PVC formulations.

The spectra of the raw materials are shown in figure 5. From this we can identify clear bands which could be used to quantify the distribution of a particular component. By using the ν(C=O) at 1650 cm^{-1} characteristic of the biocide we are able to monitor it's distribution in the polymeric matrix (figure 6(a)).

(a)

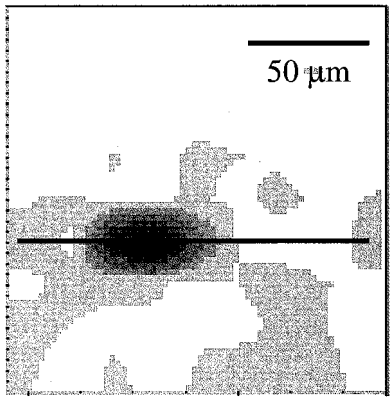

(b)

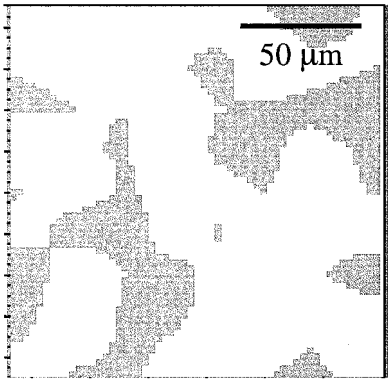

Figure 6. The distribution of biocide (5%) in a PVC formulation (a) as prepared (b) after immersion in water.

It is evident that there is a heterogeneous distribution of the concentration of biocide in the polymer matrix and this can be demonstrated spectroscopically by extracting a line map from the grey scale image (figure 7). In this figure the high intensity region in figure 6(a)

is clearly shown at around 60 μm.

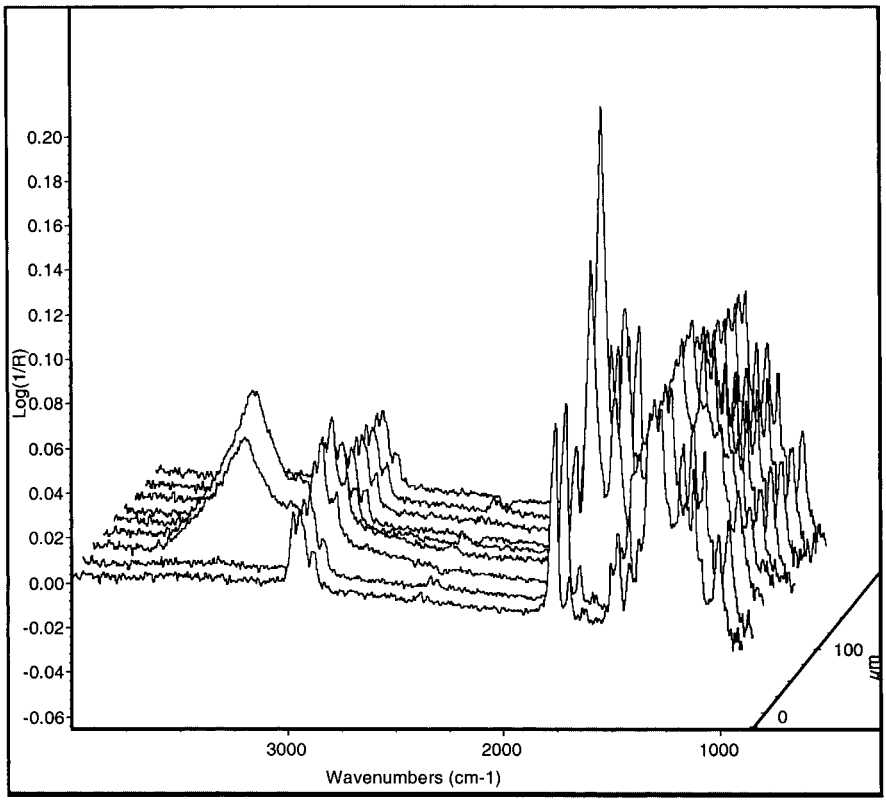

Figure 7. Line map extracted from figure 6(a) highlighting the biocide rich region. The first spectrum in this waterfall is taken from the left hand edge of the line drawn in figure 6(a).

The sample was immersed in water for 24 hours at ambient temperature, dried and the same area was 'mapped'. Figure 6(b) shows that the biocide has been redistributed. One would imagine that the process involved is 'leaching' but other data has shown this is not the case. Indeed, the biocide is only sparingly soluble in water (approximately 15 ppm).

Examination of the water after the PVC film has been immersed has shown little or no trace of biocide. What we believe is happening is that the polymer matrix is significantly swollen, creating large voids and making the movement of the biocide molecules easier. Having shown that the technique can be used to generate images of the spatial distribution of components, a formulation closer to that used in industry was examined. In this case a 0.5% loading of biocide was used. The maps of biocide distribution before and after immersion in water are shown in figure 8. Firstly, sensitivity does not appear to be an issue and secondly, a redistribution of biocide after immersion in water is once more observed.

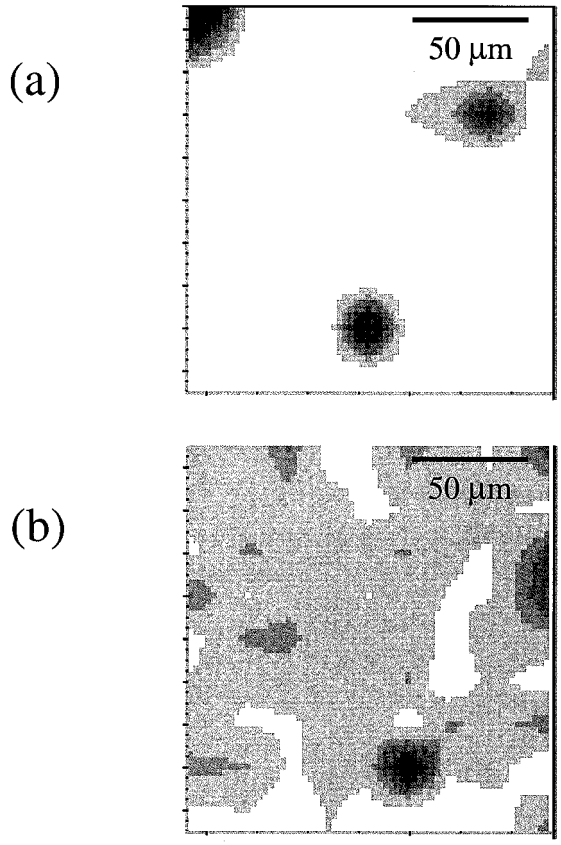

Figure 8. The distribution of biocide (0.5%) in a PVC formulation (a) as prepared (b) after immersion in water.

3 Characterising defects in PET coatings

Polymer coatings on metals are used to provide corrosion protection and/or improve the aesthetic appearance. Coatings are produced in a number of ways and occasionally defects can be found which may have an effect on the ability of a coating to carry out its purpose. We will describe the analysis of one such defect on a PET coated metal.

PET is a semi-crystalline polymer consisting of crystals in an amorphous matrix. Crystallinity in PET can be characterised in terms of the conformation of the ethylene glycol moiety [13-15]. In the crystalline state the ethylene glycol section of the molecule has been found to be in the all *trans* conformer, whilst in the amorphous state the ethylene glycol moiety has been shown to be a mixture of *trans* and *gauche* conformers [13-15]. Infrared spectroscopy can readily distinguish between crystalline and amorphous PET, as many bands are conformationally sensitive [13-15]. The CH_2 wagging modes are particularly sensitive to change, with the 1340 cm^{-1} band relating to the trans conformer and the 1370 cm^{-1} band pertaining to the 'gauche' conformer (figure 9).

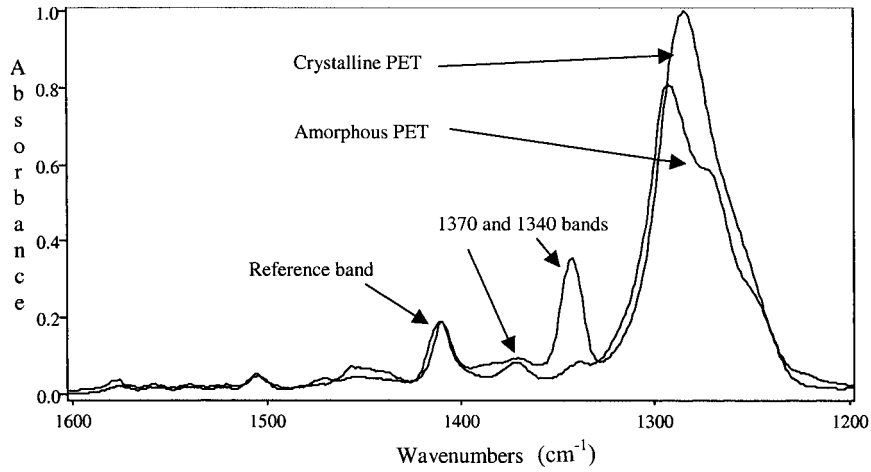

Figure 9. FTIR spectra showing the differences between highly crystalline and amorphous PET samples .

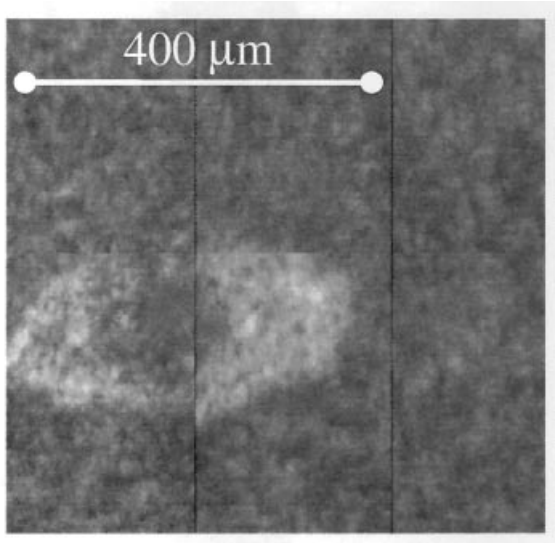

Figure 10. Optical micrograph of defect on PET coated metal.

An optical micrograph of the defect in the PET coating is shown in figure 10. FTIR-ATR microscopy was used to chemically map this defect and the resulting output is shown in figure 11(a) ATR was chosen rather than 'transflectance' in this instance as the defect was thought to be surface bound. There appears to be little information from the 'chemigram' (the integrated intensity of the whole of the spectrum shown in figure 11(a)) and spectra of the defect area (not shown) are clearly of PET. But, if one 'homes in' on the wagging modes and maps for the intensity of the 1340 cm^{-1} trans band ratioed against the 1410 cm^{-1} band (indicated in figure 9), the contrast between the 'defect' and the rest of the PET coating is evident (figure 11(b)). Indeed, the defect appears to be a region of high crystallinity, which is opaque to visible light.

Conclusions

We have demonstrated that FTIR-ATR microscopy can be used to map heterogeneity in a series of polymeric systems. It circumvents the application of time consuming sample preparation can give good molecular information about the distribution of components in mixtures. FTIR-ATR microscopy can suffer from surface topography problems, therefore only relatively smooth surfaces can be examined due to the good contact required between the ATR crystal and the sample.

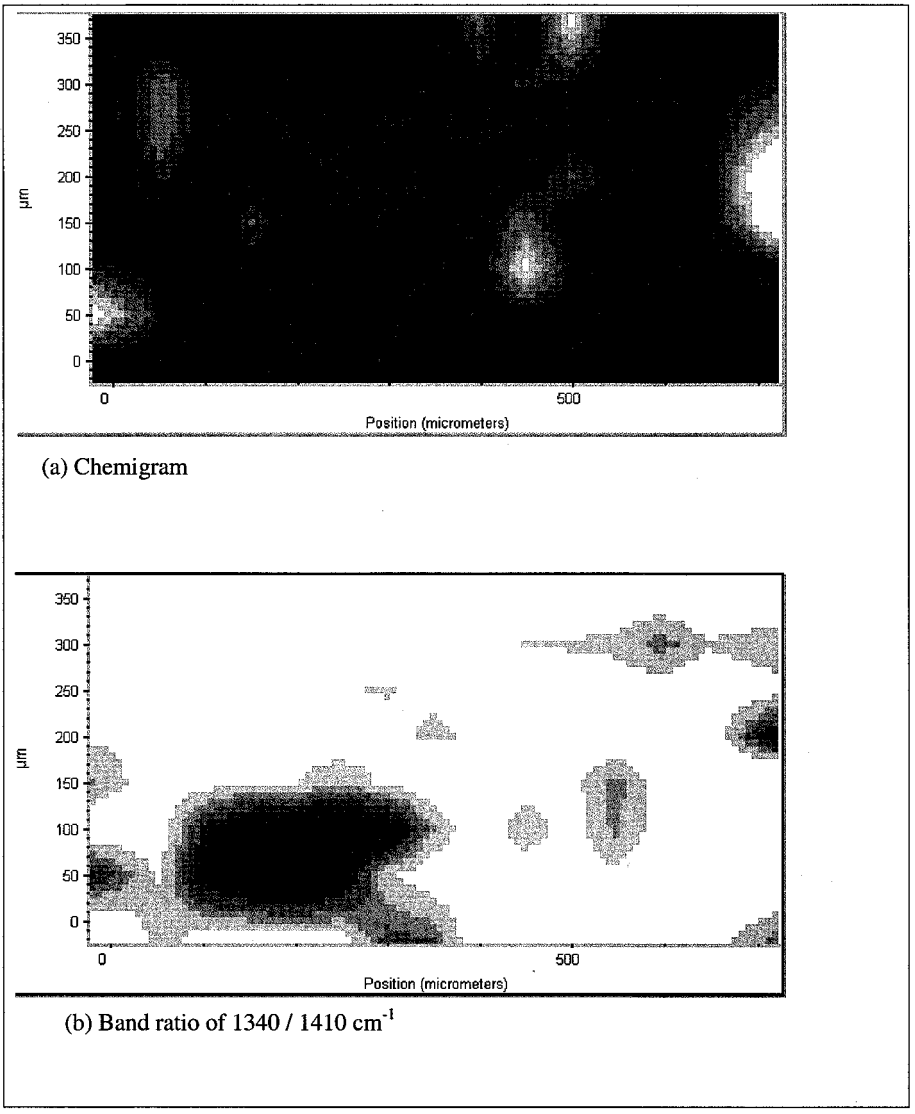

Figure 11. FTIR maps of a defect on PET coated metal (a) the integrated intensity of the whole spectrum (chemigram) and (b) the integrated intensity of the 1340 cm^{-1} trans band ratioed against the 1410 cm^{-1} band.

Acknowledgements

The equipment used in this work was purchased with the support of ERDF funding. The work was carried out with the kind support of Avecia and Corus. The authors wish to acknowledge the assistance of Prof. Jack Yarwood for the invaluable discussions during the preparation of this manuscript.

References

[1] Koenig JL, in '*Advances in polymer sciences*' vol 54, Springer Verlag, Berlin 1983

[2] Messerschmidt R, in '*Infrared spectroscopy - Theory and applications*', Marcel Dekker Inc, New York 1988

[3] Costa L, Luda P, Trossarelli L, Brach del Praver EM, Crova M and Gallinaro P, *Biomaterials* **1998**, 22, 307

[4] Costa L, Bracco P, Brach del Praver EM, Luda P and Trossarelli L, *Biomaterials* **2001**, 19, 659

[5] Celina M, Wise J, Ottesen DK, Gillen KT and Clough RL, *Polym. Degrad. Stab.* **2000,** 68, 171

[6] Am-Ende M, and Peppas N, *Pharmaceut. Res.* **1995**, 12(12), 2030

[7] Kalasinsky K, *Cell. Molec. Biol.* **1998**, 44(1), 81

[8] Chalmers JM, Everall NJ and Ellison S, *Micron* **1996**, 27(5), 315

[9] Mirabella FM, *Appl. Spectrosc. Rev.* **1985**, 21, 45

[10] Colin Melia, personal communication

[11] Summers JW, *J. Vinyl and Additive Tech.* **1997**, 3, 130

[12] Mura C, Yarwood J, Swart R and Hodge D, *Polymer* **2000**, 41, 8659

[13] Lin S-B and. Koenig JL, J. *Polym. Sci. Polym. Phys. Ed.* **1983**, 21, 2067

[14] Walls DJ, *Appl. Spec.* **1991**, 45, 7, 1193

[15] Cole KC, Guèvremont J, Ajji A and Dumoulin MM, *Appl. Spec.* **1994**, 48, 12, 1513